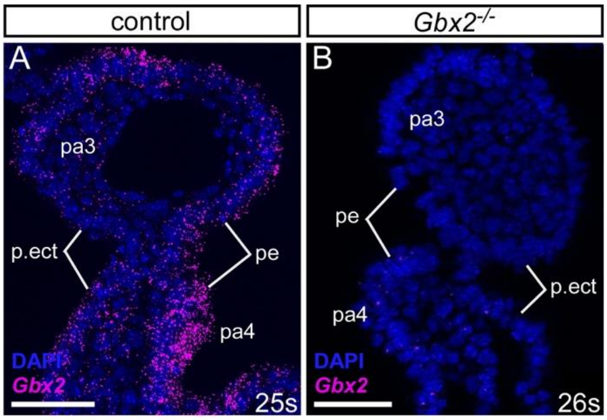

Figure S1. No *Gbx2* mRNA is detected in *Gbx2*$^{-/-}$ embryos created by recombining the *Gbx2*^{flox} allele with *Sox2Cre* at E9.5. (**A**) RNAscope in situ hybridisation shows *Gbx2* mRNA expression in the pharyngeal arch (pa) ectoderm (p.ect) and endoderm (pe) in wild-type embryos (n = 5, 24–28 somites). (**B**) No *Gbx2* mRNA is detected in *Gbx2*$^{-/-}$ embryos (n = 3, 25–27 somites). Scale bars: 50 µm. The somite numbers given in the legend reflect the range analysed for the whole study. The figure contains representative images only.

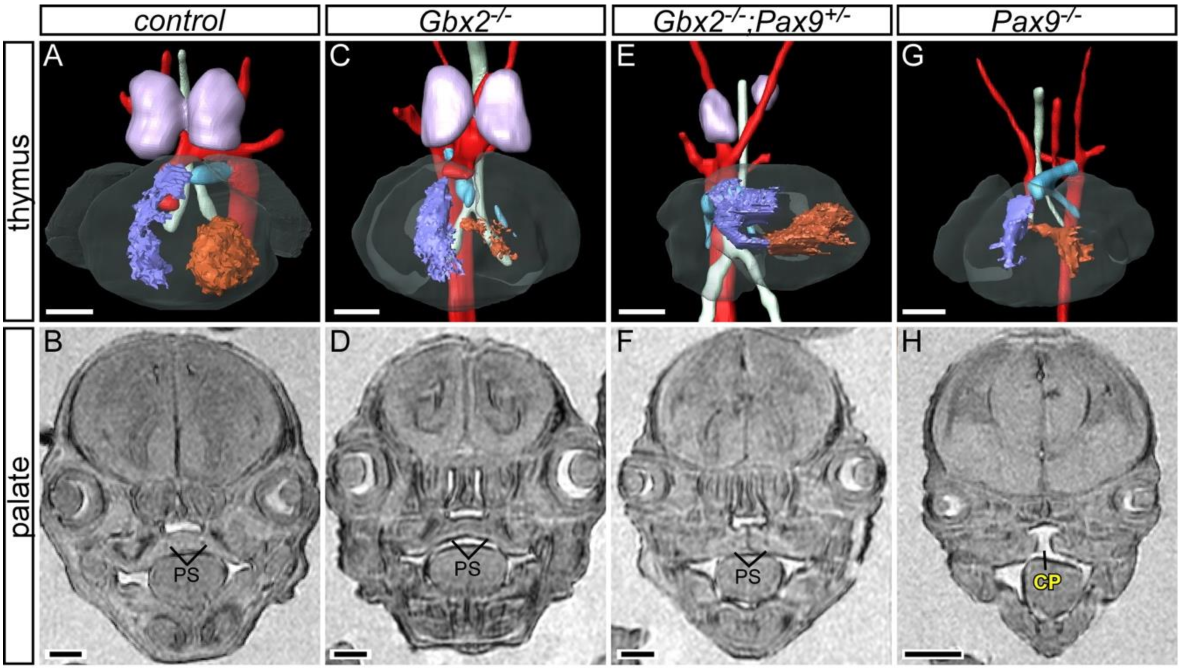

Figure S2. Thymus and palate abnormalities seen in *Gbx2;Pax9* mutant embryos and neonates. E15.5 embryos were examined by MRI. (**A**,**B**) Control embryos had normally placed thymic lobes (*purple*) located ventrally to the aortic arch arteries (**A**), and closed palatal shelves (PS; B). (**C**,**D**) Most *Gbx2*$^{-/-}$ embryos (n = 25 examined) had a normal thymus (**C**) and palate (**D**). (**E**,**F**) A large number of *Gbx2*$^{-/-}$*;Pax9*$^{+/-}$ mutants (n = 10/14 examined) had small and misplaced thymic lobes (**E**) or the thymus was absent. The palate was unaffected (**F**). (**G**,**H**) In all embryos and neonates with a *Pax9*$^{-/-}$ genotype, i.e., *Pax9*$^{-/-}$ (n = 9), *Gbx2*$^{+/-}$*;Pax9*$^{-/-}$ (n = 9), and *Gbx2*$^{-/-}$*;Pax9*$^{-/-}$ (n = 2), the thymus was absent and a cleft palate (CP) was observed. Scale, 500 µm.

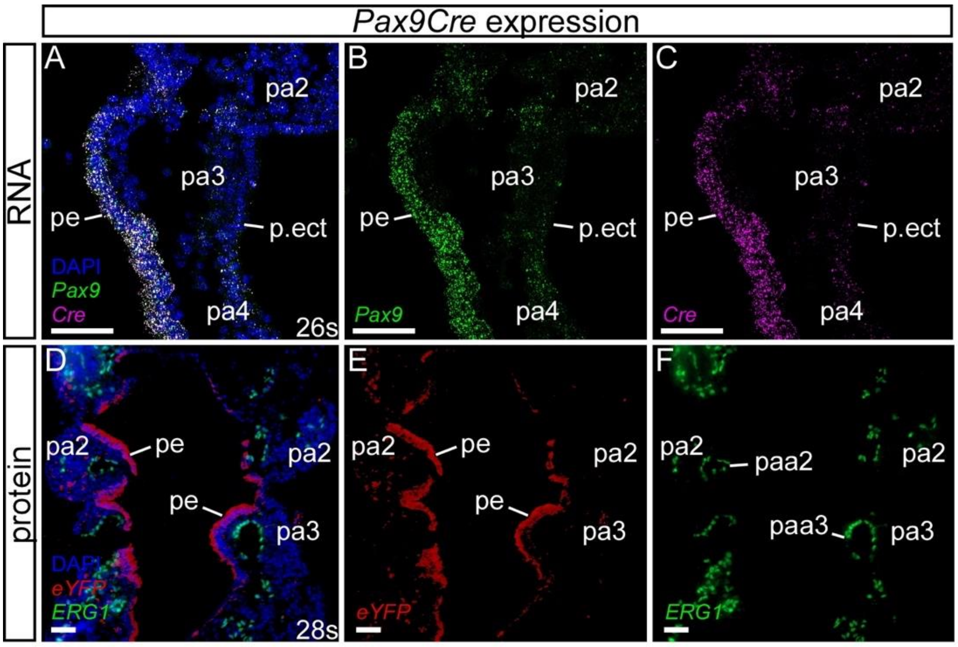

Figure S3. *Pax9Cre* activity in the pharyngeal endoderm in E9.5 embryos. (**A–C**) RNA in situ hybridisation showing *Pax9* and *Cre* expression in the pharyngeal endoderm in a *Pax9Cre* positive embryo. *Pax9* (**B**) and *Cre* expression (**C**) overlap in the pharyngeal endoderm (**A**). (**D–F**) eYFP reporter gene expression from the *Pax9Cre* allele is shown by immunostaining with an anti-eYFP antibody (red) in the pharyngeal endoderm (**D,E**). Endothelial cells have also been labelled with an anti-ERG1 antibody (**D,F**). Abbreviations: pa, pharyngeal arch; paa, pharyngeal arch artery; pe, pharyngeal endoderm; p.ect, pharyngeal ectoderm. Somite numbers are indicated (s). Scale, 50 µm.

Table S1. Expected and observed genotypes of embryos and foetuses collected from a *Gbx2*$^{+/-}$ intercross.

Genotype	Observed	Expected
Gbx2$^{+/+}$	61	67.75
Gbx2$^{+/-}$	173	135.5
Gbx2$^{-/-}$	37	67.75
Total	271	271
	Chi-square, $p = 4 \times 10^{-6}$	

Table S2. Expected and observed genotypes of weaned pups from a *Gbx2*$^{+/-}$ x *Pax9*$^{+/-}$ cross.

Genotype	Observed (3 Weeks Old)	Expected
Gbx2$^{+/+}$;*Pax9*$^{+/+}$	79	76.75
Pax9$^{+/-}$	74	76.75
Gbx2$^{+/-}$	95	76.75
Gbx2$^{+/-}$;*Pax9*$^{+/-}$	59	76.75
Total	307	307
	Chi-square, $p = 0.035$	

Table S3. Expected and observed genotypes of embryos and foetuses collected from a *Gbx2*$^{+/-}$; *Pax9*$^{+/-}$ intercross.

Genotype	Observed (E9.5-P0)	Expected
Gbx2$^{+/+}$;*Pax9*$^{+/+}$	16	10.75
Pax9$^{+/-}$	20	21.5
Gbx2$^{+/-}$	23	21.5
Pax9$^{-/-}$	9	10.75
Gbx2$^{-/-}$	5	10.75
Gbx2$^{+/-}$;*Pax9*$^{+/-}$	67	43

Gbx2$^{+/-}$;$^{-}$*Pax9*$^{-/-}$	19	21.5
Gbx2$^{-/-}$;*Pax9*$^{+/-}$	10	21.5
Gbx2$^{-/-}$;*Pax9*$^{-/-}$	3	10.75
Total	172	172
	Chi-square, $p = 1.12 \times 10^{-4}$	

Table S4. Summary of thymus phenotypes observed in *Gbx2* and *Gbx2;Pax9* mutant embryos at E15.5 and neonates at P0.

<table>
<tr><th rowspan="2">Genotype</th><th rowspan="2">Stage</th><th rowspan="2">n</th><th colspan="3">Thymus Phenotype</th></tr>
<tr><th>Normal</th><th>Split/
Asymmetric/
Vestigial</th><th>Absent</th></tr>
<tr><td>Gbx2^{−/−}</td><td>E15.5</td><td>25</td><td>23
(92%)</td><td>2
(8%)</td><td>0</td></tr>
<tr><td rowspan="2">Gbx2^{−/−};Pax9^{+/−}</td><td>E15.5</td><td>13</td><td rowspan="2">4
(28%)</td><td rowspan="2">4***
(28%)</td><td rowspan="2">6***
(43%)</td></tr>
<tr><td>P0</td><td>1</td></tr>
<tr><td rowspan="2">Pax9^{−/−}</td><td>E15.5</td><td>7</td><td rowspan="2">0</td><td rowspan="2">0</td><td rowspan="2">9
(100%)</td></tr>
<tr><td>P0</td><td>2</td></tr>
<tr><td rowspan="2">Gbx2^{+/−};Pax9^{−/−}</td><td>E15.5</td><td>7</td><td rowspan="2">0</td><td rowspan="2">0</td><td rowspan="2">9
(100%)</td></tr>
<tr><td>P0</td><td>2</td></tr>
<tr><td rowspan="2">Gbx2^{−/−};Pax9^{−/−}</td><td>E15.5</td><td>1</td><td rowspan="2">0</td><td rowspan="2">0</td><td rowspan="2">2
(100%)</td></tr>
<tr><td>P0</td><td>1</td></tr>
</table>

The thymus was significantly more frequently seen to be asymmetric in appearance and split apart, or absent, in *Gbx2*$^{-/-}$;*Pax9*$^{+/-}$ mutants compared to *Gbx2*$^{-/-}$ mutants (***$p < 0.0001$, Fisher's exact test). An abnormal thymus was always associated with an arch artery defect.

Table S5. Antibodies and probes used for immunostaining and in situ hybridisation.

<table>
<tr><th>Target</th><th>Catalogue Number</th><th>Species and Type</th><th>Supplier</th><th>Dilution</th></tr>
<tr><td colspan="5">Primary antibody</td></tr>
<tr><td>ERG1</td><td>ab92513</td><td>Rabbit monoclonal</td><td>Abcam</td><td>1:1000</td></tr>
<tr><td colspan="5">Secondary antibody</td></tr>
<tr><td>Donkey anti-rabbit IgG
Alexa Fluor 594</td><td>A-21207</td><td>-</td><td>Thermo Fisher
Scientific</td><td>1:200</td></tr>
<tr><td colspan="5">Nuclear stain</td></tr>
<tr><td>DAPI</td><td>H-1200</td><td>-</td><td>Vector Laboratories</td><td>-</td></tr>
<tr><td colspan="5">RNAscope probes</td></tr>
<tr><td>Pax9</td><td>454321-C2</td><td rowspan="3">Mouse</td><td rowspan="3">Advanced Cell
Diagnostics</td><td>1:50</td></tr>
<tr><td>Tbx1</td><td>481911</td><td>Direct</td></tr>
<tr><td>Gbx2</td><td>314358</td><td>1:50</td></tr>
</table>